Interpretation of Penetration Resistance for Back-analysis at Sites of Previous Liquefaction

Scott M. Olson
URS Corporation

Stephen F. Obermeier
EqLiq Consulting

Timothy D. Stark
University of Illinois at Urbana-Champaign

INTRODUCTION

Liquefaction and paleoliquefaction studies are being used increasingly to interpret ground motion parameters (*i.e.*, acceleration distribution, earthquake magnitude, and epicentral location) in regions of the world that experience infrequent, but damaging, earthquakes. These studies are especially applicable when the most recent damaging earthquakes occurred prior to the development of ground-motion instrumentation. For example, Martin and Clough (1994) examined liquefaction features formed during the 1886 Charleston, South Carolina earthquake; Pond (1996) and Obermeier and Pond (1999) examined paleoliquefaction features formed during a number of paleoearthquakes in the Wabash Valley region along the Indiana–Illinois border; Dickenson and Obermeier (1998) and Obermeier and Dickenson (2000) examined paleoliquefaction features formed during the 1700 Cascadia earthquake of the Pacific Northwest; and Ellis and de Alba (1999) recently examined liquefaction features formed during the 1755 Cape Ann, Massachusetts earthquake.

Many of these studies back-calculate seismic parameters using the results of penetration tests conducted long after the earthquake. The most common method to back-calculate a lower-bound peak ground surface acceleration is to use the lowest value of penetration resistance obtained at a historic or paleoliquefaction site in conjunction with a correlation for liquefaction resistance of sandy soils, *e.g.*, Seed *et al.* (1985) or Stark and Olson (1995). In some studies, the current value of penetration resistance is assumed to be the "representative" value for back-analysis (*e.g.*, Pond, 1996), while in other studies corrections are made to the current value of penetration resistance prior to back-analysis (*e.g.*, Ellis and de Alba, 1999).

This paper examines some of the factors that affect the interpretation of a "representative" penetration resistance for back-analysis of seismic parameters. The interpretation of these factors is illustrated using an example historic liquefaction site. The back-calculated values of a_{max} from the example case history show the sensitivity of the back-analysis to the interpretation of penetration resistance. Brief descriptions of soil mechanics terms used herein are provided in Appendix I. More detailed descriptions of many of these terms can be found in Terzaghi *et al.* (1996).

EXAMPLE CASE HISTORY

Ellis and de Alba (1999) used a site that experienced level ground liquefaction during the 1755 Cape Ann earthquake to estimate the minimum peak horizontal ground surface acceleration (minimum a_{max}) required to cause the ground failure. This case history involved the eruption of sand blows in the town of Scituate, Massachusetts. Ellis and de Alba (1999) reported the results of standard penetration tests (SPT's) that were conducted in 1995 adjacent to the liquefaction site. The soil profile, $(N_1)_{60}$ values (SPT blowcount corrected to an energy ratio of 60% and an effective overburden stress of approximately 100 kPa), and fines content (percentage of soil by weight passing the U.S. standard #200 sieve) are reproduced from Ellis and de Alba (1999) in Figure 1.

As noted by Ellis and de Alba (1999), the $(N_1)_{60}$ values below 13 feet average around 10 blows per foot (bpf). However, the fines content increases from near zero at a depth of 11 feet to greater than 30% at a depth of 24 feet. Liquefac-

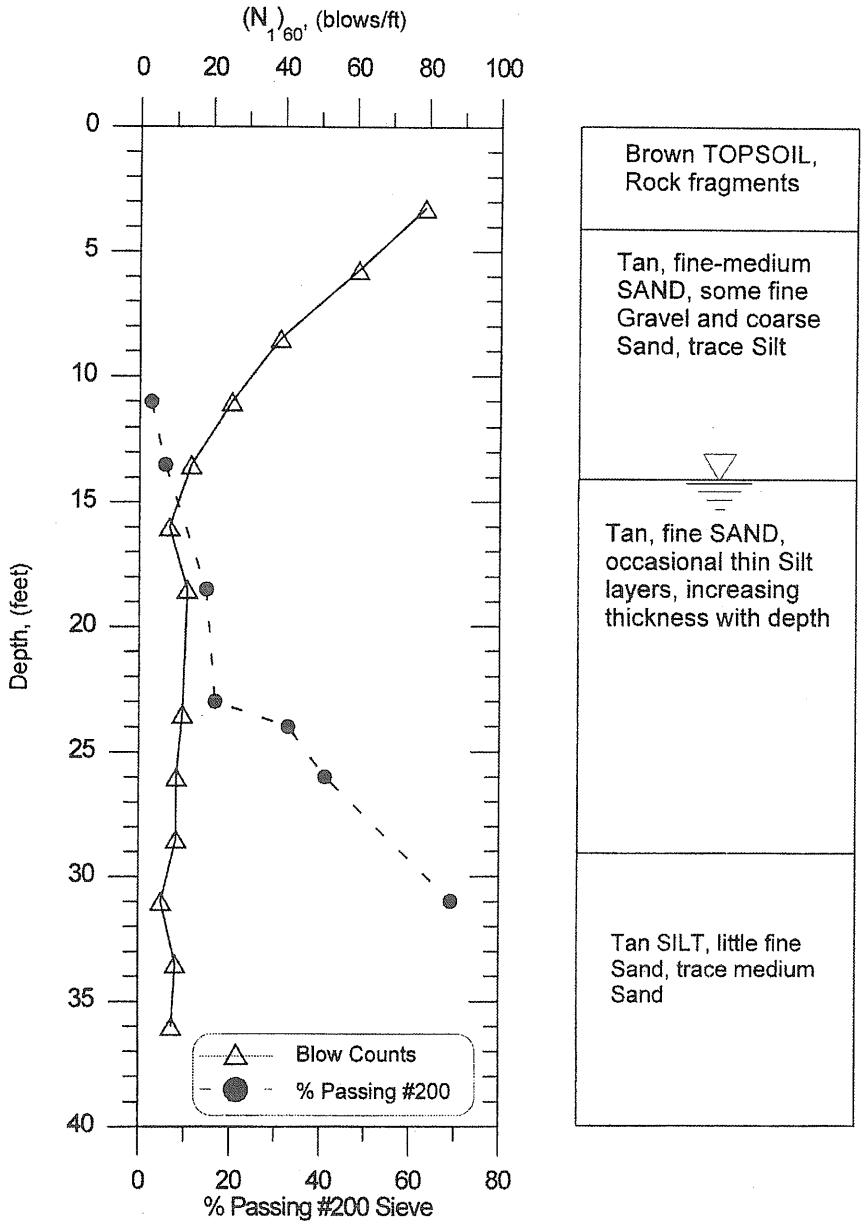

▲ **Figure 1.** Soil description, $(N_1)_{60}$ values, and fines content versus depth for boring conducted adjacent to historic liquefaction site, Bailey House, Scituate, Massachusetts (from Ellis and de Alba, 1999).

tion resistance relationships (*e.g.*, Seed *et al.*, 1985 and Stark and Olson, 1995) indicate that at a given value of penetration resistance, resistance to liquefaction increases with increasing fines content. Therefore, Ellis and de Alba (1999) concluded that the sandy soils between approximately 13 and 23 feet are most vulnerable to liquefaction. For calculation of the seismically induced shear stresses required for back-analysis, Ellis and de Alba (1999) decreased the depth to the water table by 2 feet (from 14 feet to 12 feet) to account for the seasonal variation.

Ellis and de Alba (1999) concluded that the $(N_1)_{60}$ value of 8 bpf measured at a depth of 16 feet (fines content at this depth is 12%) is the critical value for back-analysis of the minimum a_{max} (see Figure 1). Therefore, this value is used as the *current* (actually measured in 1995) value of blowcount.

FACTORS AFFECTING THE INTERPRETATION OF PENETRATION RESISTANCE

The determination of the representative blowcount for back-analysis depends on the interpretation of the relative effects of the following factors: (1) destruction of pre-earthquake soil structure and aging effects during liquefaction; (2) postliquefaction consolidation and densification; and (3) postliquefaction aging. In addition, consideration must be given to how the liquefaction analysis procedure was devel-

oped and how it should be applied for back-analysis, *e.g.*, should the pre- or postearthquake values of penetration resistance be used.

Use of Pre- or Postearthquake Blowcount

When developing the original liquefaction resistance relationships, Seed and Idriss (1971), Seed *et al.* (1975), and Seed (1979) used considerable judgment in their interpretation of field SPT blowcount values to account for the effects of liquefaction and earthquake shaking. In other words, Seed and his colleagues attempted to correct the postearthquake blowcounts to pre-earthquake conditions so that *predictive* liquefaction resistance relationships could be developed. These relationships are used to predict the occurrence or nonoccurrence of liquefaction at any site (P. de Alba, written comm., 2000). Therefore, Ellis and de Alba (1999) indicated that pre-earthquake blowcounts should be used to back-analyze seismic parameters to be consistent with the original intent of the liquefaction resistance relationships.

However, the SPT and cone penetration test (CPT) databases of level ground liquefaction and nonliquefaction cases that are now used for liquefaction resistance relationships consist almost exclusively of cases where penetration resistance was measured *after* the causative earthquake (T. L. Youd, written comm., 1999; Olson and Stark, 1998). These values of penetration resistance have not been modified in any way for the effects of liquefaction or earthquake shaking. The updated SPT-based level ground liquefaction resistance relationships developed by Seed *et al.* (1985) as modified by Youd and Idriss (1997) are presented in Figure 2. To be consistent with these updated relationships, the postearthquake blowcount should be used for back-analysis of seismic parameters. The difference between using the pre-earthquake versus postearthquake penetration resistance to back-analyze a_{max} can be significant, as illustrated subsequently.

Destruction of Pre-Earthquake Soil Structure due to Liquefaction

As succinctly stated by Schmertmann (1991), "Soils age." Following deposition, natural and man-made deposits develop a structure resulting from postdepositional mechanical readjustment (secondary compression) and possible weak chemical bonding at particle contacts. This process is referred to as aging. The development of soil structure results in the improvement of soil properties such as shear strength, modulus, and penetration resistance (Schmertmann, 1991).

Thomann and Hryciw (1992) suggest that liquefaction causes effectively infinite shear straining at particle contacts, which completely destroys the soil structure. As a result, the soil essentially becomes freshly deposited following postliquefaction consolidation. Because liquefaction destroys the pre-earthquake soil structure and aging effects, penetration resistance immediately following liquefaction may decrease, despite an increase in density that usually results from postliquefaction consolidation. In other words, immediately following liquefaction and the dissipation of seismically induced porewater pressures, the deposit may have a *lower* penetration resistance compared to its pre-earthquake penetration resistance. Mesri *et al.* (1990) presented data showing this effect as the result of blast-induced liquefaction and vibrocompaction. An example of this behavior is shown in Figure 3 following blast densification at Jebba Dam (Mesri *et al.*, 1990). In Figure 3, $[q_c]_0$ and $[q_c]_R$ are the CPT tip resistances measured prior to and at some reference time following blast densification, respectively. (These values will be used in Figure 5 subsequently.) The average q_c values measured at two depth intervals (27–28 m [open squares] and 32–33 m [open circles]) at various times with respect to the individual blasts are plotted in Figure 3. The average q_c values at both depths clearly show an immediate decrease in penetration resistance following the first blast and show a lower postblasting penetration resistance for approximately 90 days following the first blast and 30 days following the third blast. This decrease in penetration resistance immediately following blast-induced liquefaction is in contrast to the increase in penetration resistance following liquefaction suggested by Ellis and de Alba (1999).

Postliquefaction Consolidation and Densification

Seismic liquefaction results from an increase in porewater pressure induced by earthquake shaking. The subsequent dissipation of these excess porewater pressures (*i.e.*, consolidation) results in an overall densification of a liquefied deposit. Goto (1968) documented both increases and decreases in field (uncorrected) blowcounts following the 1964 Niigata earthquake. Figure 4 presents the data collected by Goto (1968) as solid circles. Based on these data, Goto (1968) concluded that contractive (loose) sands contract/densify (*i.e.*, blowcount increases) and dilative (dense) sands expand/loosen (*i.e.*, blowcount decreases) during earthquake shaking. However, based on data collected by Shahien (1998), presented in Figure 4 as open circles, the trend observed by Goto (1968) does not appear to be general. The reason the trend observed by Goto (1968) is not verified by the data in Figure 4 may be related to the destruction of soil structure during liquefaction, the magnitude of postliquefaction densification, and the elapsed time between the occurrence of liquefaction and the blowcount measurement. The authors note that contractive and dilative behavior are influenced by not only density but also effective stress. However, the data presented in Figure 4 generally correspond to cases where the vertical effective stress was in the range of 50 to 150 kPa. This is also the typical range of vertical effective stress reported for most level ground liquefaction case histories (see Seed *et al.*, 1985; Olson and Stark, 1998). For this range of vertical effective stress, sands with low blowcounts (*i.e.*, loose sands with $N \leq 10$) typically are contractive, and sands with high blowcounts (*i.e.*, medium dense to dense sands with $N > \sim 20$) typically are dilative.

As aforementioned, an increase in density occurs as seismically induced excess porewater pressures dissipate. Seed *et al.* (1989) concluded that an increase in relative density of

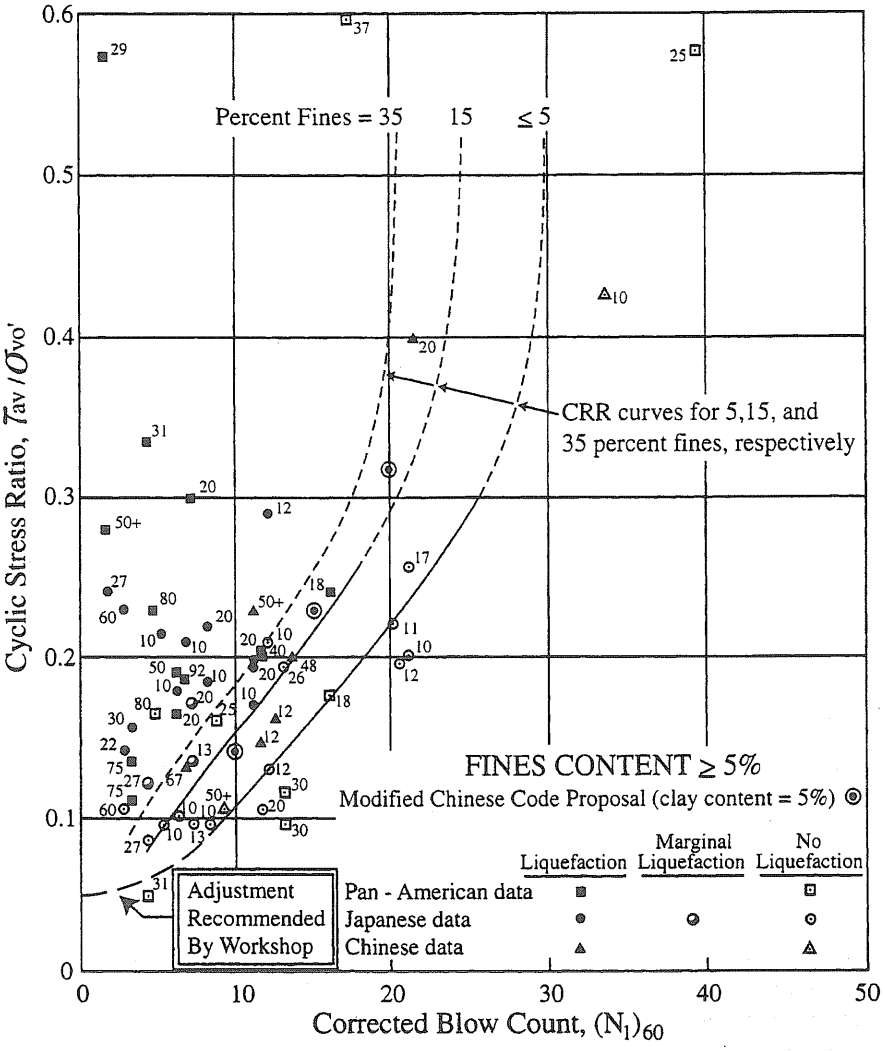

▲ **Figure 2.** SPT-based liquefaction resistance relationships for sandy soils (from Youd and Idriss, 1997).

approximately 4% occurred in the silty sands of the downstream shell of Lower San Fernando Dam as a result of shaking during the 1971 San Fernando earthquake. The magnitude of density change due to liquefaction at other sites will depend on the pre-earthquake relative density of the deposit (Shahien, 1998), as well as on the site conditions, severity of liquefaction, and duration of strong shaking. However, because of the destruction of the pre-earthquake soil structure, postliquefaction densification may not result in an increase in blowcount immediately after the earthquake.

Mesri *et al.* (1990) summarized available data on the change in penetration resistance measured 1 to 30 days after densification, as shown in Figure 5. The parameter $\Delta e_R = \Delta e / (e_{max} - e_{min})$ is the change in void ratio (Δe) normalized by the maximum possible change in void ratio ($e_{max} - e_{min}$). The value of Δe_R is equivalent to ΔD_r (change in relative density resulting from postliquefaction consolidation). As illustrated in Figure 5, values of postdensification q_c, $[q_c]_R$, are lower than predensification q_c values, $[q_c]_0$, for small increases in relative density or void ratio for values of $[q_c]_R$ measured 1 to 30 days following densification.

Figure 5 also indicates that two different penetration resistance conditions can result following liquefaction. The first condition results when the change in relative density following liquefaction is small. In this case, the penetration resistance measured shortly after completion of postliquefaction consolidation is smaller than the pre-earthquake value. This suggests that the effect of destruction of pre-earthquake soil structure on penetration resistance is larger than the effect of densification. This would generally correspond to cases of relatively marginal development of liquefaction or for situations where aging has occurred for a long period of time (on the order of hundreds to thousands of years) prior to liquefaction and densification. The second condition results when the relative density change following liquefaction is large. Here, the postdensification penetration resistance is larger than the pre-earthquake value. The data in Figure 5 suggest that for large increases in relative density, the effect of the increase in relative density on penetration

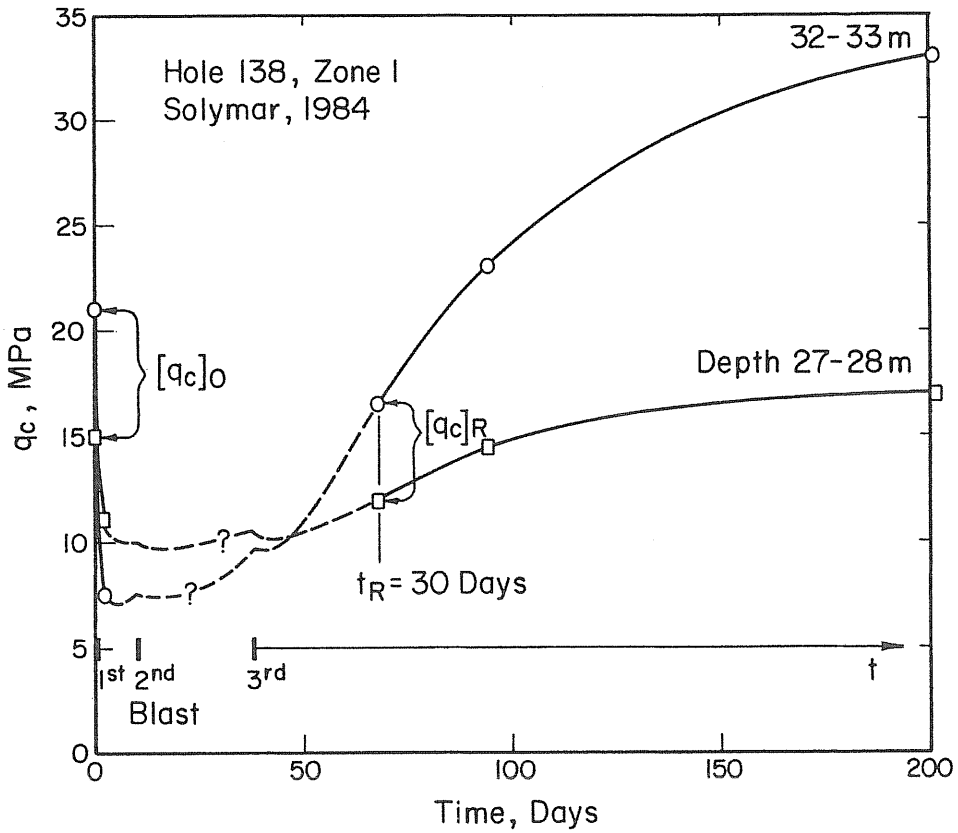

▲ **Figure 3.** Measured q_c behavior with time after blast-densification at Jebba Dam showing initial decrease in penetration resistance resulting from destruction of soil structure and subsequent increase in penetration resistance resulting from drained soil aging (from Mesri *et al.*, 1990).

resistance is greater than the effect of destruction of soil structure. This condition likely corresponds to cases of severe liquefaction that involve large quantities of ejecta, high levels and/or long durations of shaking, or when aging has occurred for a short period of time (on the order of tens to hundreds of years) prior to liquefaction and densification.

The data in Figure 4 likely consist of cases corresponding to both conditions. This helps explain the lack of a well defined trend between pre- and postearthquake penetration resistance values. The authors anticipate that the SPT and CPT databases used to develop liquefaction resistance relationships (*e.g.*, Figure 2) are skewed toward an increased postearthquake penetration resistance (*i.e.*, the latter condition above) because the large majority of the data were obtained from regions of frequent strong earthquakes. However, a decreased postearthquake penetration resistance following liquefaction (*i.e.*, the former condition above) may be more common in regions such as the eastern and central U.S. where large earthquakes are infrequent, which allows significant aging between earthquakes.

In contrast, Ellis and de Alba (1999) suggested that postliquefaction densification should result in an increase in blowcount, and the increase $[\Delta(N_1)_{60(\text{densification})}]$ for the Scituate, Massachusetts site can be estimated from

$$\Delta(N_1)_{60(\text{densification})} = 110 \cdot D_r \cdot \Delta D_r \quad (1)$$

where D_r is the pre-earthquake relative density of the deposit. This equation was adapted from Seed *et al.* (1989) from the study of Lower San Fernando Dam. The equation was developed by taking the derivative (with respect to relative density) of the following equation developed by Skempton (1986):

$$(N_1)_{60} = c \cdot D_r^2 \quad (2)$$

where c is a constant that depends on several factors, including median particle diameter, overconsolidation ratio, and age of the deposit. Values of c will be evaluated subsequently.

Postliquefaction or Postdepositional Aging

Mesri *et al.* (1990) indicated that freshly deposited or densified clean sands exhibit substantial increases in stiffness, horizontal stress, and penetration resistance during secondary compression under drained conditions. Schmertmann (1987) suggested that the penetration resistance increases following densification result from time-dependent recovery of horizontal stresses and frictional gain in modulus and strength, which are caused by particle reorientation during secondary compression. Mesri *et al.* (1990) further explained that "the increase in stiffness and in effective horizontal stress result from continued rearrangement of sand particles resulting in an enhanced macro-interlocking of sand grains and

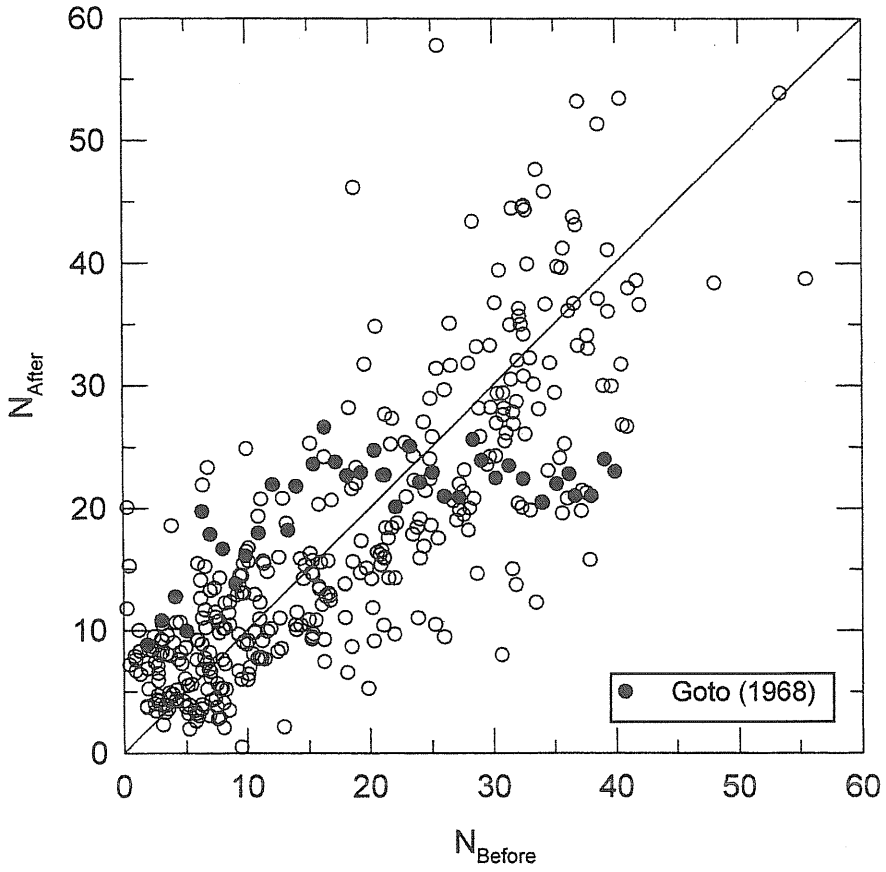

▲ **Figure 4.** Comparison of SPT blowcounts measured before and after earthquake shaking (from Shahien, 1998).

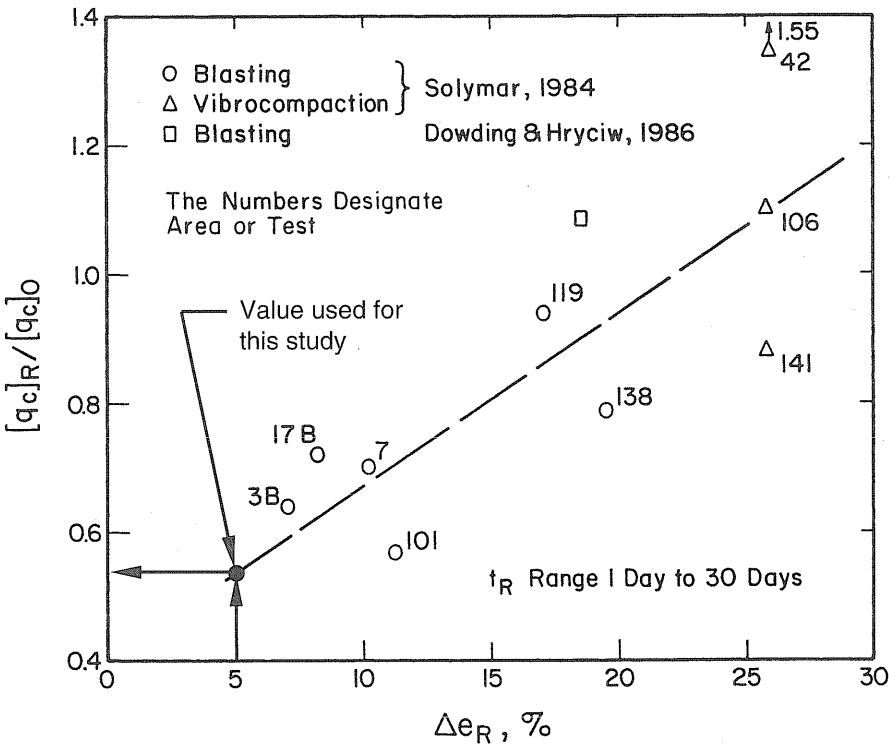

▲ **Figure 5.** Ratio of postdensification q_c value (measured 1 to 30 days after densification) to predensification q_c value for different areas and densification procedures (from Mesri *et al.*, 1990).

micro-interlocking of grain surface roughness." Therefore, with certain notable exceptions, it is likely that a substantial portion of the increase in penetration resistance over short geologic time periods (say, at least hundreds of years) results from secondary compression, not chemical precipitation or bonding.

Mesri *et al.* (1990) suggested the following equation to estimate the increase in CPT penetration resistance following densification resulting from secondary compression only:

$$\frac{q_c}{(q_c)_R} = \left(\frac{t}{t_R}\right)^{C_D C_\alpha / C_c} \tag{3}$$

where $(q_c)_R$ is a reference cone penetration resistance at a reference time t_R following deposition or densification, q_c is the cone penetration resistance at any time $t > t_R$, C_D is a parameter that reflects the densification effect, and C_α/C_c is the ratio of secondary compression index to compression index. As both CPT and SPT penetration resistances are affected similarly by soil compressibility and horizontal effective stress, it seems reasonable to substitute N_{60} for q_c in Equation (3). For values of penetration resistance compared at the same depth, *i.e.*, same vertical effective stress, it also is reasonable to substitute $(N_1)_{60}$ for N_{60}. This substitution results in:

$$\frac{(N_1)_{60}}{[(N_1)_{60}]_R} = \left(\frac{t}{t_R}\right)^{C_D C_\alpha / C_c} \tag{4}$$

Using cone penetration test data obtained before and after cases of blast densification, vibrocompaction, and dynamic compaction, Mesri *et al.* (1990) proposed the trends shown in Figure 6 to estimate C_D on the bases of the densification procedure and the magnitude of relative density increase.

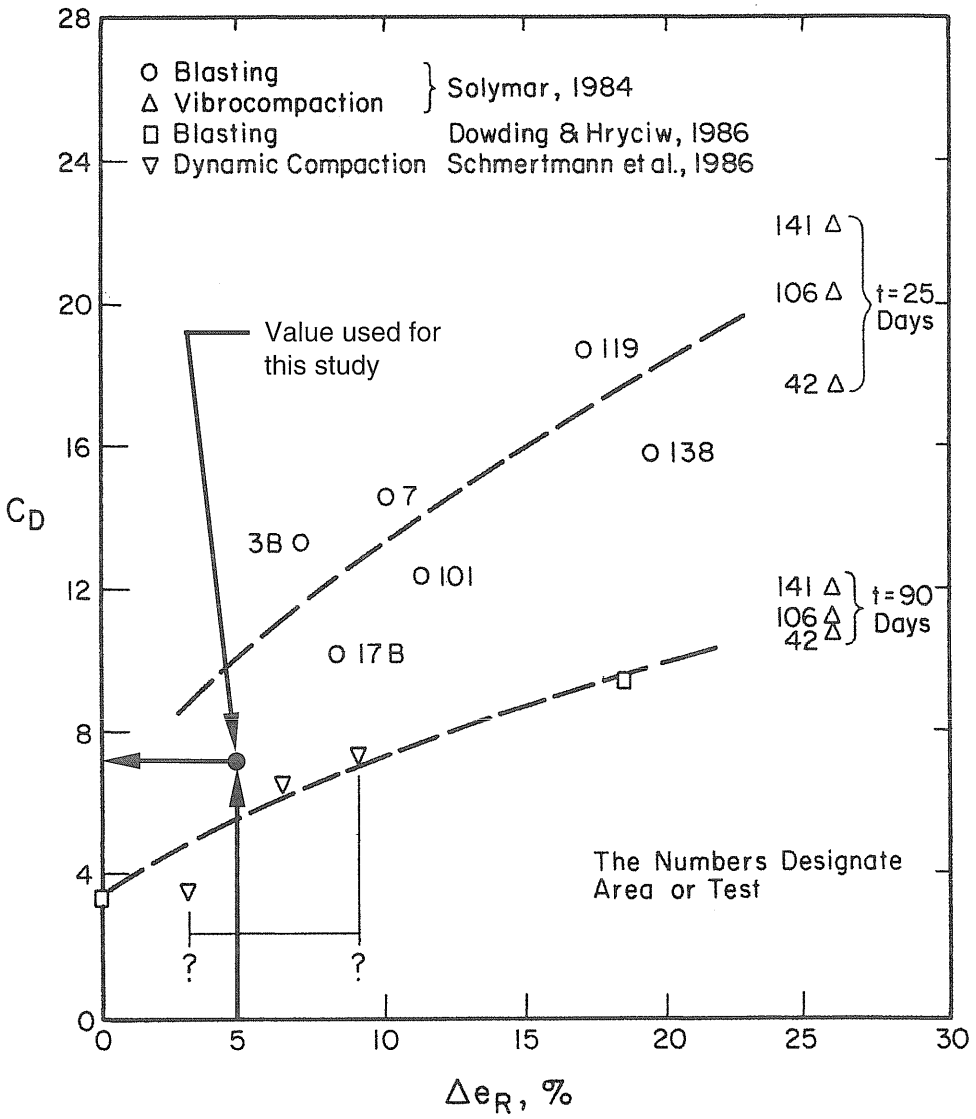

▲ **Figure 6.** Summary of C_D data for ground modification/densification projects (from Mesri *et al.*, 1990).

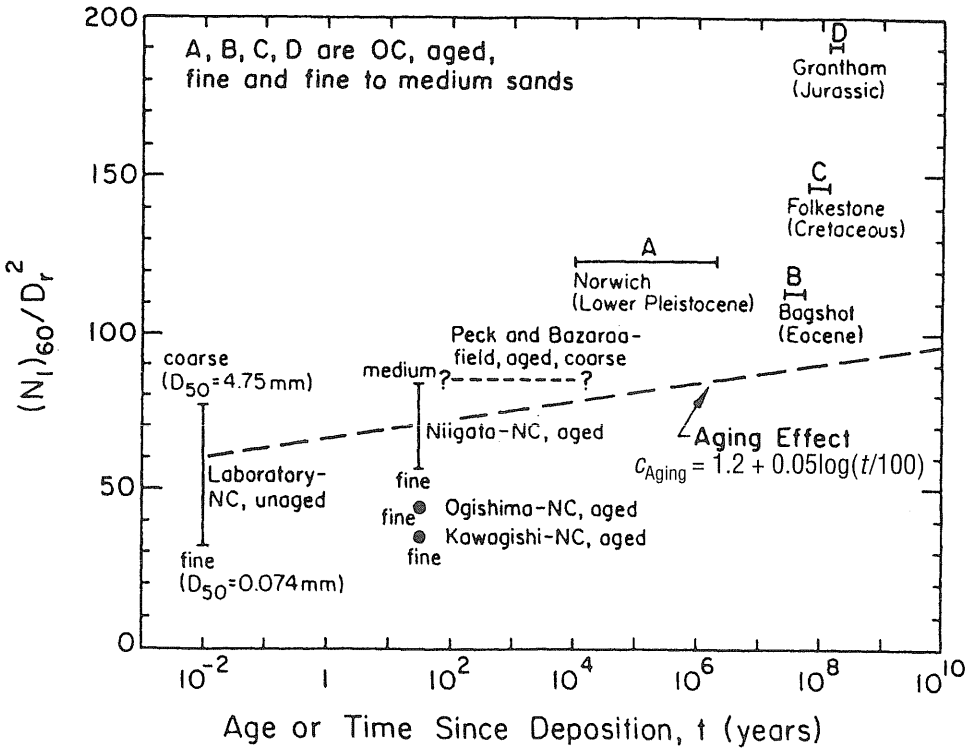

▲ **Figure 7.** Aging effect on blowcount for sands (from Kulhawy and Mayne, 1990).

The use of Figure 6 and Equation (4) provides a rough estimate of the increase in penetration resistance with time resulting from postdensification or postliquefaction aging.

Alternatively, the effect of aging following liquefaction can be estimated using the relationship proposed by Kulhawy and Mayne (1990). Kulhawy and Mayne (1990) re-evaluated data from Skempton (1986) and incorporated other data available in the literature to develop the relationship between c and deposit age shown in Figure 7, where the aging effect, c_{Aging}, is estimated as:

$$c_{Aging} = 1.2 + 0.05 \log\left(\frac{t}{100}\right) \tag{5}$$

and c from Equation (2) is estimated as:

$$c = c_P \cdot c_{Aging} \tag{6}$$

where c_P relates $(N_1)_{60}$ to D_r^2 for freshly deposited sandy soils as a function of median particle diameter. Values of c, c_P, and c_{Aging} for the example case history are evaluated subsequently.

In the short term, it is likely that secondary compression is the dominant factor that influences aging, while over geologic time chemical cementation may become significant. The authors suspect that chemical factors may have increased the measured blowcounts of the sands in Figure 7 older than about 1,000 years. Therefore, Equation (5) probably is applicable for times less than 1,000 years, with certain notable exceptions.

INTERPRETATION OF PENETRATION RESISTANCE

The effects of soil structure destruction, postliquefaction densification, and postliquefaction aging can be combined in several ways to form at least five scenarios for estimating the "representative" blowcount to be used for back-analysis of the Scituate, Massachusetts case history. These five scenarios are:

1. Use the blowcount immediately prior to the earthquake by decreasing the blowcount for aging from 1995 to 1755 (postearthquake) using Equation (4) and Figure 6 and adjust blowcount to account for destruction of soil structure and densification resulting from liquefaction (*i.e.*, postearthquake 1755 to pre-earthquake 1755) using Figure 5.
2. Use the blowcount immediately prior to the earthquake by decreasing the blowcount for aging from 1995 to 1755 (postearthquake) using Equation (5) and decrease blowcount to account for densification resulting from liquefaction (*i.e.*, postearthquake 1755 to pre-earthquake 1755) using Equation (1), neglecting the effect of destruction of soil structure. This is the procedure used by Ellis and de Alba (1999), although Ellis and de Alba (1999) made a different interpretation of Equation (2) to develop their blowcount corrections.

TABLE 1
Interpretations of $(N_1)_{60}$ for Back-Calculation of a_{max}/g

Scenario[a]	Parameters for the Mesri *et al.* (1990) procedure					Parameters for the Kulhawy and Mayne (1990) procedure			$(N_1)_{60}$ at given Time			τ_{ave}/σ'_{vo}		a_{max}/g	
	Δe_R (%)	$[(N_1)_{60}]_R/[(N_1)_{60}]_0$	C_α/C_c	C_D	t_R (years)	c_P[b]	c_{Aging}	c[c]	Current (1995) $(N_1)_{60}$	Postearthquake (1755) $[(N_1)_{60}]_R$	Preearthquake (1755) $[(N_1)_{60}]_0$	$(M_s = 7.5)$	$(M_s = 7.5)$	$(M_s = 7.5)$	$(M_s = 6.0)$
1	5	0.55	0.02	7	0.15	—	—	—	8	~3	5	0.09		0.13	0.17
2	—	—	—	—	—	45	1.22	55	8	~7	6	0.10		0.15	0.19
3	5	0.55	0.02	7	0.15	—	—	—	8	3	—	0.07		0.10	0.12
4	—	—	—	—	—	45	1.22	55	8	7	—	0.12		0.17	0.22
5	—	—	—	—	—	—	—	—	8	—	8	0.13		0.18	0.24
Ellis and de Alba (1999)	—	—	—	—	—	55	1.4	77	8	~6	4	0.08		0.11	0.14

a. Descriptions of various scenarios are provided in text.
b. Parameter accounting for median particle diameter.
c. $c = c_P \cdot c_{Aging}$

3. Use the blowcount immediately after the earthquake by decreasing the blowcount for aging from 1995 to 1755 (postearthquake) using Equation (4) and Figure 6.
4. Use the blowcount immediately after the earthquake by decreasing the blowcount for aging from 1995 to 1755 (postearthquake) using Equation (5).
5. Use the current (1995) blowcount, assuming that the effect of postliquefaction aging has been negligible.

Figure 8 and Table 1 present timelines of changes in blowcount during the time period from pre-earthquake 1755 to 1995 for each scenario described above. Included in Figure 8 and Table 1 are the assumptions made by Ellis and de Alba (1999) to determine the "representative" blowcount. The procedure and calculations for each timeline are described below.

Scenario 1. Correction for Postliquefaction Aging and Destruction of Soil Structure

This scenario decreases the current (1995) blowcount for 240 years of postliquefaction aging using the Mesri *et al.* (1990) procedure, *i.e.*, Equation (4) and Figure 6. This provides an estimate of the postearthquake blowcount. The postearthquake blowcount then is adjusted for destruction of the soil structure using Figure 5 to obtain the pre-earthquake blowcount. Mesri *et al.* (1990) suggested $C_D \approx 7$ (see Figure 6) and $C_\alpha/C_c = 0.02$ (see Figure 2 of Mesri *et al.*, 1990 for a compilation of C_α/C_c data for clean sands) for general cases of densification and subsequent aging of sandy soils. The value of Δe_R, equivalent to ΔD_r, was estimated by Ellis and de Alba (1999) to be around 4 – 5%. Using $\Delta e_R = 5\%$ and the midrange of the trendlines results in $[q_c]_R/[q_c]_0$ of approximately 0.55 (see Figure 5). As indicated previously, it is assumed that $[q_c]_R/[q_c]_0 \approx [(N_1)_{60}]_R/[(N_1)_{60}]_0$. The reference time, t_R, in Equation (4) was selected as 0.15 years for simplicity and because all postliquefaction consolidation should be complete within 0.15 years for the deposit evaluated. The penetration resistance timeline for this scenario is shown in Figure 8(a) and Table 1.

Scenario 2. Correction for Aging and Densification Resulting from Consolidation

This scenario also decreases the current (1995) blowcount for 240 years of postliquefaction aging, except it uses the Kulhawy and Mayne (1990) relationship shown in Equation (5). An average value of $c_P = 45$ was obtained from the two relationships presented in Figure 9. Correcting the value of c_P for aging over 240 years (by multiplying by c_{Aging} of 1.22) results in $c = 55$. Using $c = 55$ and the *current aged* $(N_1)_{60}$ of 8 in Equation (2) provides a postearthquake D_r of 38%. Assuming an increase in D_r of 5% due to densification (Ellis and de Alba, 1999) provides a pre-earthquake D_r of 33%. These values of c, pre-earthquake D_r, and ΔD_r were used in Eqs. (1) and (2) to estimate the pre-earthquake value of blowcount shown in Figure 8(b) and Table 1.

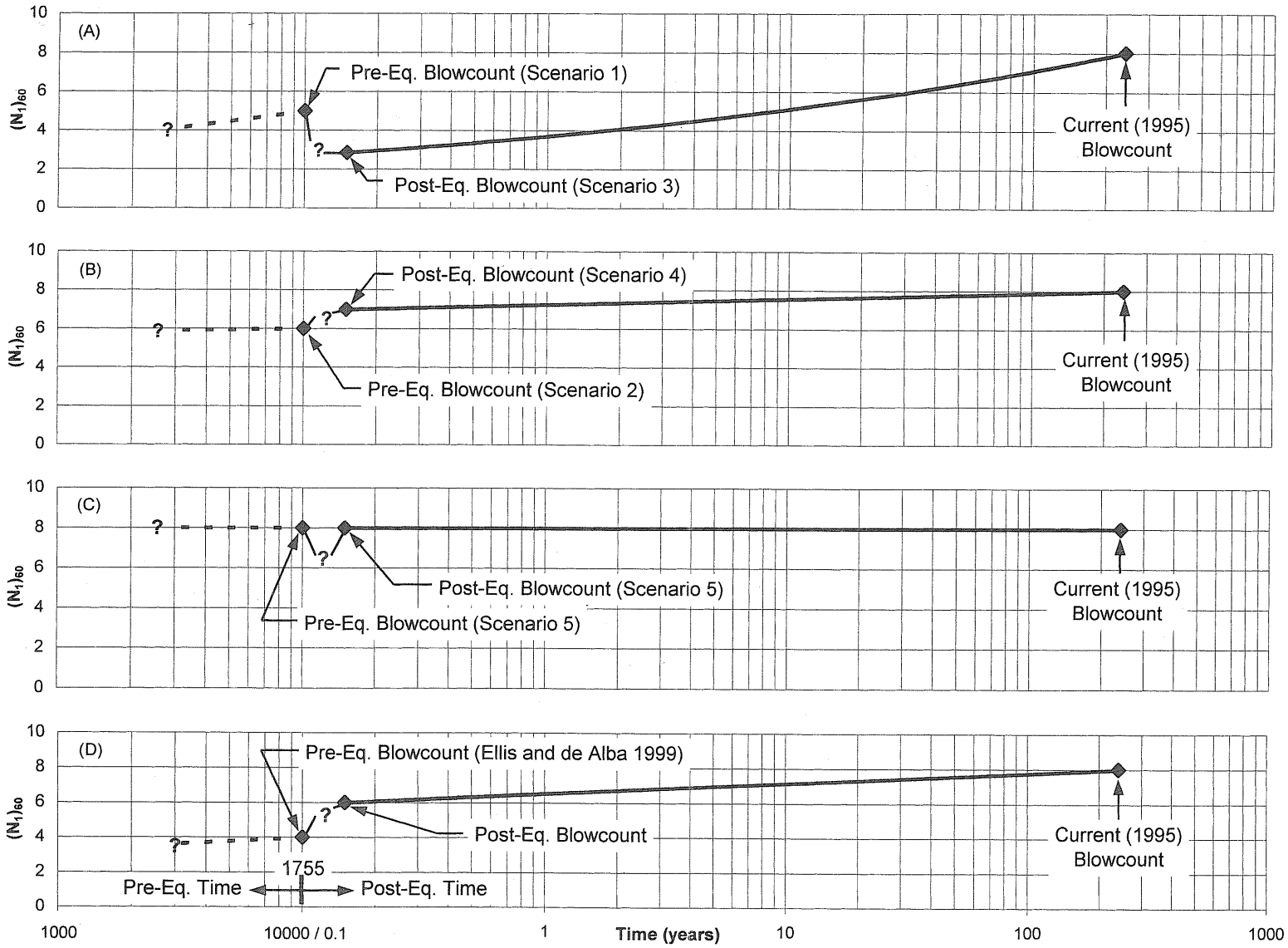

▲ **Figure 8.** Timelines of corrected SPT blowcount for times before and after 1755 earthquake.

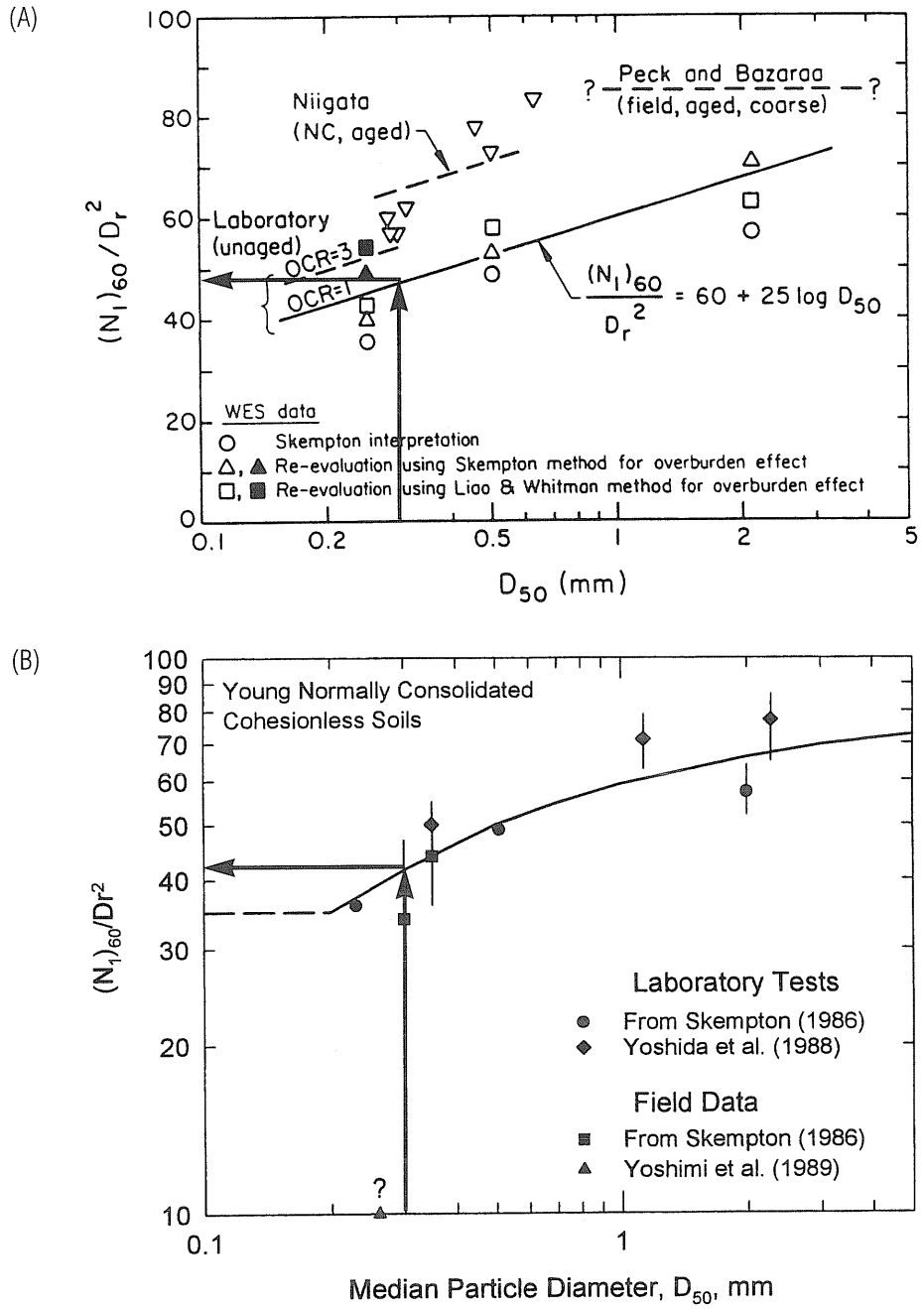

▲ **Figure 9.** Relationships between $(N_1)_{60}/D_r^2$ and median particle diameter for normally consolidated young cohesionless soils from (A) Kulhawy and Mayne (1990) and (B) Shahien (1998).

This procedure was also used by Ellis and de Alba (1999); however, Ellis and de Alba (1999) interpreted the values of c and c_{Aging} differently than described above. Their interpretations and the resulting penetration resistance timeline are shown in Figure 8(d) and Table 1.

Scenario 3. Correction for Aging Only (Mesri *et al.*, 1990 Procedure)

This scenario is identical to Scenario 1, except it excludes the correction for destruction of soil structure. The resulting penetration resistance timeline for this scenario also is shown in Figure 8(a) and Table 1.

Scenario 4. Correction for Aging Only (Kulhawy and Mayne, 1990 Procedure)

This scenario can be evaluated in two ways. First, Equation (2) can be used to determine the postliquefaction $(N_1)_{60}$ by incorporating a value of $c = c_p = 45$ for freshly deposited silty sand (which corresponds to 1755 postliquefaction conditions, when c_{Aging} is negligible) and the postliquefaction $D_r = 38\%$ estimated in Scenario 2. Alternatively, the value of

c_{Aging} of 1.22 (for 240 years of aging) suggests that aging increases the value of $(N_1)_{60}$ by 22%. Either using Equation (2) or reducing the current (1995) blowcount by 22% results in a postliquefaction $(N_1)_{60}$ of about 7, as shown in Figure 8(b) and Table 1.

Scenario 5. No Correction to *Current* (1995) Blowcount

Under certain geologic conditions, aging may have a minor effect on postliquefaction penetration resistance. One such condition may be sandy soils with a large component of carbonates, as encountered in the Wabash Valley of Illinois–Indiana. Over time, the carbonates may be dissolved and removed by the groundwater flow, reducing the effect of aging on penetration resistance. Another setting with no apparent effects of aging is the nearly pure quartz sands of coastal South Carolina (Martin and Clough, 1994). The reason(s) for the absence of aging in this setting is not clear at this time.

Alternatively, the deposit at Scituate, Massachusetts, prior to the 1755 earthquake, had likely been subjected to other earthquakes widely spaced in time throughout its geologic history, and, even if not, the deposit is 10,000 to 15,000 years old (de Alba, written comm., 2000) and would have experienced considerable aging over this time. Therefore, the sand deposit *prior* to the earthquake was already aged, and no correction would be required to adjust the current (1995) aged deposit to its pre-earthquake (1755) aged condition. The resulting penetration resistance timeline for this scenario is shown in Figure 8(c) and Table 1.

In summary, these arguments suggest that there is considerable uncertainty in correcting the value of $(N_1)_{60}$ for loss of pre-earthquake soil structure, postliquefaction densification, and postliquefaction aging. Clearly the relative importance of each of these factors is dependent on local site and seismic conditions. Additional research is required to better understand how each of these factors are affected by local site and seismic conditions. However, with judgment, a range of back-calculated values of peak horizontal ground surface acceleration can be estimated in many field settings as shown below.

BACK-CALCULATED VALUES OF a_{max}/g

Table 1 also presents the back-calculated values of a_{max}/g for the various interpretations of blowcount. The "simplified" equation (Seed and Idriss, 1971; Seed *et al.*, 1985) was used for the back-calculation:

$$\frac{\tau_{ave}}{\sigma'_{vo}} = 0.65 \frac{a_{max}}{g} \frac{\sigma_{vo}}{\sigma'_{vo}} r_d \qquad (7)$$

where τ_{ave}/σ'_{vo} is the average cyclic stress ratio required to trigger liquefaction, σ_{vo} is the vertical total stress, σ'_{vo} is the vertical effective stress, and r_d is a depth reduction factor. Values of τ_{ave}/σ'_{vo} were obtained from the SPT-based silty sand liquefaction resistance relationship (fines content ~15%, see Figure 2) and values of σ_{vo}/σ'_{vo} and r_d were obtained from Ellis and de Alba (1999). To correct this cyclic stress ratio to an earthquake magnitude of 6.0, values of τ_{ave}/σ'_{vo} were increased by 30% (as suggested by Ellis and de Alba, 1999).

The back-calculated values of a_{max}/g range from 0.12 to 0.24. These values are approximately 15% lower to 70% higher than the best estimate of 0.14 suggested by Ellis and de Alba (1999). Further, all of the values fall within the range of acceleration values observed for the inferred modified Mercalli intensity (Kramer, 1996) of VII reported by Ellis and de Alba (1999). While this variation in a_{max}/g is considered reasonable given the uncertainties involved, this exercise illustrates the uncertainty inherent in the interpretation of a "representative" blowcount and back-analysis of seismic parameters from liquefaction case histories. It should also be noted that the back-calculation of a_{max} using Equation (7) at a single site provides only a lower-bound value of a_{max}, because only the minimum value of $(N_1)_{60}$ from the soil profile (see Figure 1) can be certain to have liquefied. Therefore, underestimating a_{max} at this step may lead to a considerable underestimate of the actual value of a_{max}.

CONCLUSIONS

Seismic parameters, such as peak ground surface acceleration (a_{max}), can be back-calculated from historic or prehistoric liquefaction sites. One common back-calculation method employs existing liquefaction resistance relationships to estimate the minimum value of a_{max} required to trigger liquefaction at a site. This back-calculation procedure depends on the value of penetration resistance considered representative of the liquefied layer. However, the penetration resistance may necessarily be measured long after the causative earthquake. Therefore, the "representative" penetration resistance for back-calculation must be interpreted in terms of the relative effects of the following factors: (1) destruction of pre-earthquake soil structure during liquefaction; (2) postliquefaction consolidation and densification; and (3) postliquefaction aging. In addition, consideration must be given to how the engineering analysis procedures were developed and how they should be applied for back-analysis, *e.g.*, should the pre- or postliquefaction value of penetration resistance be used.

Various interpretations of these factors lead to considerably different back-calculated values of a_{max}. For the example historic liquefaction site examined herein, back-calculated values of a_{max} ranged from 0.12 g to 0.24 g. Despite this considerable range, these values are in agreement with the range of values observed in other earthquakes at the same value of modified Mercalli intensity. Therefore, considerable judgment must be used when interpreting the "representative" penetration resistance to be used for back-calculation. Further, the uncertainty involved in any such back-calculation should be understood and highlighted. At this time, it seems prudent to evaluate each of these factors on a site-specific basis and estimate a range of a_{max}, rather than a single value.

ACKNOWLEDGMENTS

This study was funded by the National Science Foundation (NSF), Grant Number 97-01785, as part of the Mid-America Earthquake (MAE) Center headquartered at the University of Illinois at Urbana-Champaign. This support is gratefully acknowledged. The authors would also like to thank Professor Pedro de Alba and the anonymous reviewers for their insightful reviews of this manuscript.

REFERENCES

de Alba, P. (2000). Written communication to the authors regarding the interpretation of blowcount used in Ellis and de Alba (1999).

Dickenson, S. E. and S. F. Obermeier (1998). Ground motions estimates for a Cascadia earthquake from liquefaction evidence, *Proceedings, ASCE Specialty Conference on Geotechnical Earthquake Engineering and Soil Dynamics III*, August 3–6, Seattle, Washington, **1**, 79–90.

Dowding, C. H. and R. D. Hyrciw (1986). A laboratory study of blast densification of saturated sand, *J. of Geotechnical Eng.* **112**, 187–199.

Ellis, C. and P. de Alba (1999). Acceleration distribution and epicentral location of the 1755 "Cape Ann" earthquake from case histories of ground failure, *Seism. Res. Lett.* **70**, 758–773.

Goto, H. (1968). Damage to civil engineering construction: Electric power facilities, in Kawasumi, H. and committee (eds.), *General Report on the Niigata Earthquake of 1964*, 517–524.

Kramer, S. L. (1996). *Geotechnical Earthquake Engineering*, Prentice-Hall, Upper Saddle River, NJ, 653 pp.

Kulhawy, F. H. and P. W. Mayne (1990). Manual on estimating soil properties for foundation design, *EPRI EL-6800, Res. Proj. 1493-6, Final Report*, Electric Power Research Institute, Palo Alto, CA.

Martin, J. R. and G. W. Clough (1994). Seismic parameters from liquefaction evidence, *J. of Geotechnical Eng.* **120**, 1,345–1,361.

Mesri, G., T. W. Feng, and J. M. Benak (1990). Postdensification penetration resistance of clean sands, *J. of Geotechnical Eng.* **116**, 1,095–1,115.

Obermeier, S. F. and E. C. Pond (1999). Issues in using liquefaction features for paleoseismic analysis, *Seism. Res. Lett.* **70**, 34–58.

Obermeier, S. F. and S. E. Dickenson (2000). Liquefaction evidence for the strength of ground motions resulting from late Holocene subduction earthquakes, with emphasis on the event of 1700 AD, *Bull. Seism. Soc. Am.* **90**, 876–896.

Olson, S. M. and T. D. Stark (1998). CPT based liquefaction resistance of sandy soils, *Proc., Specialty Conf. on Geotechnical Earthquake Engineering and Soil Dynamics III*, Vol. 1, 325–336.

Pond, E. C. (1996). Seismic parameters for the central United States based on paleoliquefaction evidence in the Wabash Valley, Ph.D. Thesis, Virginia Polytechnic Institute, Blacksburg, Virginia, 583 pp.

Schmertmann, J. H. (1987). Discussion of "Time-dependent strength in freshly deposited or densified sand," by J.K. Mitchell and Z.V. Solymar, *J. of Geotechnical Eng.* **113**, 173–175.

Schmertmann, J. H. (1991). The mechanical aging of soils, *J. of Geotechnical Eng.* **117**, 1,288–1,330.

Schmertmann, J. H., F. Baker, R. Gupta, and K. Kessler (1986). CPT/DMT QC of ground modification at a power plant, *Proceedings, In Situ '86*, 985–1,001.

Seed, H. B. (1979). Soil liquefaction and cyclic mobility evaluation for level ground during earthquakes, *J. of the Geotechnical Eng. Div.* **105**, 201–255.

Seed, H. B., I. Arango, and C. K. Chan (1975). *Evaluation of Soil Liquefaction Potential during Earthquakes*, Report No. EERC 75-28, Earthquake Engineering Research Center, University of California, Berkeley, CA.

Seed, H. B. and I. M. Idriss (1971). Simplified procedure for evaluating soil liquefaction potential, *J. of the Soil Mechanics and Foundations Div.* **97**, 1,249–1,273.

Seed, H. B., R. B. Seed, L. F. Harder, and H.-L. Jong (1989). *Re-evaluation of the Lower San Fernando Dam: Report 2, Examination of the Post-earthquake Slide of February 9, 1971*, U.S. Army Corps of Engineers Contract Report GL-89-2, U.S. Army Corps of Engineers Waterways Experiment Station, Vicksburg, MS.

Seed, H. B., K. Tokimatsu, L. F. Harder, and R. Chung (1985). Influence of SPT procedures in soil liquefaction resistance evaluations, *J. of the Geotechnical Eng. Div.* **111**, 861–878.

Shahien, M. M. (1998). Settlement of Structures on Granular Soils Subjected to Static and Earthquake Loads, Ph.D. thesis, University of Illinois at Urbana-Champaign, Urbana, Illinois, 1,204 pp.

Skempton, A. W. (1986). Standard penetration test procedures and the effects in sand of overburden pressure, relative density, particle size, aging, and overconsolidation, *Geotechnique* **36**, 425–447.

Solymar, Z. V. (1984). Compaction of alluvial sands by deep blasting, *Canadian Geotechnical J.* **21**, 305–321.

Stark, T. D. and S. M. Olson (1995). Liquefaction resistance using CPT and field case histories, *J. of Geotechnical Eng.* **121**, 856–869.

Terzaghi, K., R. B. Peck, and G. Mesri (1996). *Soil Mechanics in Engineering Practice, Third Edition*, John Wiley & Sons, Inc., New York, 549 pp.

Thomann, T. G. and R. D. Hryciw (1992). Discussion of "Postdensification penetration resistance of clean sands," by G. Mesri, T.W. Feng, and J.M. Benak, *J. of Geotechnical Eng.* **118**, 508–511.

Yoshida, Y., M. Ikemi, and T. Kokusho (1988). Empirical formulas of SPT blowcounts for gravelly soils, in De Ruiter, J. (ed.), *Proceedings, First International Symposium on Penetration Testing*, Orlando, Florida, **1**, 381–387.

Yoshimi, Y., K. Tokimatsu, and Y. Hosaka (1989). Evaluation of liquefaction resistance of clean sands based on high-quality undisturbed samples, *Soils and Foundations* **29**, 93–104.

Youd, T. L. (1999). Written communication to the authors regarding the timing of SPT tests that are used in the SPT-based level ground liquefaction case history database available at www.et.byu.edu/ce/faculty/youd/data.html.

Youd, T. L. and I. M. Idriss (1997). Summary report, *Proceedings, NCEER Workshop on Evaluation of Liquefaction Resistance of Soils*, NCEER-97-0022, 1–40.

URS Corporation
2318 Millpark Drive
Marland Heights, MO 63043
+1-314-429-0100
scott_olson@urscorp.com
(S. M. O.)

EqLiq Consulting
Rockport, IN 47635
sobermei@yahoo.com
(S. F. O.)

Department of Civil and Environmental Engineering
University of Illinois at Urbana-Champaign
Urbana, IL 61801
+1-217-333-7394
s-olson4@uiuc.edu
t-stark1@uiuc.edu
(T. D. S.)

APPENDIX I

Notations and Definitions

a_{max}	peak horizontal ground surface acceleration
bpf	# of blows measured per foot of penetration in the standard penetration test
c	Relationship between $(N_1)_{60}/D_r^2$ accounting for median particle diameter, overconsolidation ratio, and deposit age
c_{Aging}	Factor to increase c_p for effect of deposit age
c_p	Relationship between $(N_1)_{60}/D_r^2$ accounting for normally consolidated young cohesionless soils accounting only for median particle diameter
C_c	Compression index = $\Delta e / \Delta \log \sigma'_v$
C_D	Parameter that reflects any densification by vibration, blasting, liquefaction, etc., that is not related to ideally static increase in vertical effective stress
C_α	Secondary compression index = $\Delta e / \Delta \log t$ during secondary compression
CPT	Cone penetration test
CRR	Cyclic resistance ratio
D_r	Relative density (state of packing) of cohesionless soil = $(e_{max} - e)/(e_{max} - e_{min})$
e	Void ratio, *i.e.*, volume of soil voids/volume of soil solids
e_{max}	Void ratio of soil sample in loosest state as measured in laboratory
e_{min}	Void ratio of soil sample in densest state as measured in laboratory
$(N_1)_{60}$	Standard penetration test blowcount corrected to an energy ratio of 60% and an effective overburden stress of approximately 100 kPa
$[(N_1)_{60}]_0$	SPT-corrected blowcount measured prior to liquefaction or densification
$[(N_1)_{60}]_R$	SPT-corrected blowcount measured at some reference time following liquefaction or densification
q_c	CPT tip resistance
$[q_c]_0$	CPT tip resistance measured prior to liquefaction or densification
$[q_c]_R$	CPT tip resistance measured at some reference time (usually less than 30 days) following liquefaction or densification
r_d	Reduction factor to seismic shear stress computed assuming rigid body ground response to account for flexibility of soil column
SPT	Standard penetration test
t	Elapsed time
t_R	Reference time following liquefaction or densification before the measurement of penetration resistance
ΔD_r	Change in relative density resulting from postliquefaction consolidation
Δe_R	Change in void ratio resulting from postliquefaction consolidation or densification
$\Delta(N_1)_{60(densification)}$	Change in SPT blowcount resulting from postliquefaction consolidation
σ'_{vo}	Vertical effective stress
σ_{vo}	Vertical total stress
τ_{ave}	Equivalent average uniform shear stress pulse produced by an earthquake